

Recent Studies on Hypernuclei Lifetimes from STAR

Yue Hang Leung^{1,*}, for the STAR collaboration

¹University of Heidelberg

Abstract. The hyperon-nucleon (Y - N) interaction is an essential ingredient in the description of the equation-of-state of high-baryon-density matter. Light hypernuclei ($A = 3, 4$), being simple Y - N bound states, serve as cornerstones of our understanding of the Y - N interaction. Thus, precise measurements of their lifetimes are important, as they provide stringent tests to hyperon-nucleon interaction models.

The yields of light hypernuclei are expected to increase from high to low energy heavy-ion collisions due to the increase in baryon density. As a result, the STAR Beam Energy Scan II program, which spans an energy range of $\sqrt{s_{NN}} = 3.0 - 27.0$ GeV, is particularly suited for hypernuclei studies. In these proceedings, recent results on the lifetimes of light hypernuclei (${}^3_{\Lambda}\text{H}$, ${}^4_{\Lambda}\text{H}$, ${}^4_{\Lambda}\text{He}$) measured in $\sqrt{s_{NN}} = 3.0$ and 7.2 GeV Au+Au collisions are presented. The relative branching ratio R_3 of the ${}^3_{\Lambda}\text{H}$ is intimately related to its lifetime. A new R_3 measurement using data from $\sqrt{s_{NN}} = 3.0$ GeV Au+Au collisions is reported. These results will be compared to previous measurements and theoretical calculations, and the physics implications will be discussed.

1 Introduction

Hypernuclei are nuclei containing at least one hyperon. They serve as important experimental probes to access the hyperon-nucleon (Y - N) interaction, which is an important component in the equation-of-state of high-baryon-density matter, such as neutron stars. Measurements of the lifetimes and binding energies of hypernuclei provide tests for hyperon-nucleon interaction models. In particular, the hypertriton, ${}^3_{\Lambda}\text{H}$, the lightest known hypernuclei, has a small binding energy ($B_{\Lambda} \sim O(0.1$ MeV)). Due to its loosely bounded nature, it is believed that the ${}^3_{\Lambda}\text{H}$ lifetime $\tau({}^3_{\Lambda}\text{H})$ is very close to the free Λ lifetime $\tau(\Lambda)$, 263 ± 2 ps [1]. Recently, STAR, ALICE and HyPHI have reported ${}^3_{\Lambda}\text{H}$ lifetimes ranging from $\sim 50\%$ to $\sim 100\%$ of $\tau(\Lambda)$ with large uncertainties. This situation calls for more precise measurements of the ${}^3_{\Lambda}\text{H}$ lifetime to clarify the situation.

2 Hypernuclei Reconstruction with the STAR Detector

In heavy-ion collisions, hypernuclei yields are expected to increase towards lower beam energies due to the increasing baryon density [2]. The STAR Beam Energy Scan II program

*e-mail: leung@physi.uni-heidelberg.de

15 (BES-II), which covers collision energies from $\sqrt{s_{NN}} = 3.0$ to 27.0 GeV, provides a great
 16 opportunity for studies of light hypernuclei.

17 At STAR, hypernuclei are reconstructed using their mesonic decay channels, e.g. ${}^3_{\Lambda}\text{H} \rightarrow$
 18 ${}^3\text{He} + \pi^-$, ${}^4_{\Lambda}\text{He} \rightarrow {}^3\text{He} + \text{p} + \pi^-$. Particle identification of the daughter tracks is achieved
 19 by the measured ionization energy loss in the Time Projection Chamber (TPC). The KFP
 20 particle package [3], based on the Kalman Filter method, is utilized to reconstruct hypernuclei
 21 candidates from their daughter tracks. The combinatorial background is estimated via event
 22 mixing or rotating all daughter pion candidates within one event [4]. In the following, we
 23 will discuss recent hypernuclei lifetime and relative branching ratio results from STAR.

24 3 Hypernuclei Lifetimes

25 3.1 Measurements from BES-II

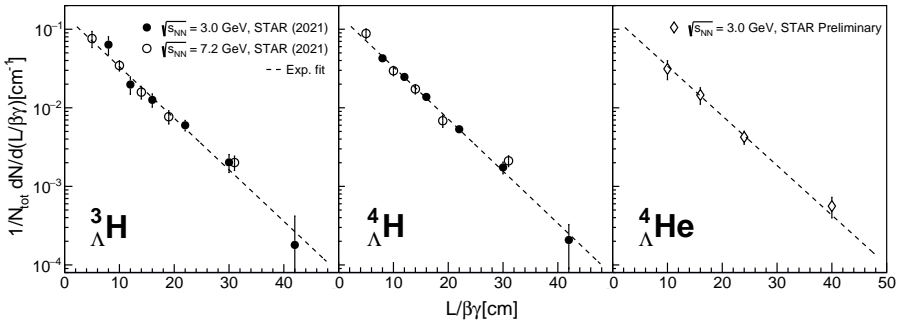


Figure 1. The normalized yield versus the proper decay length $L/\beta\gamma$ for ${}^3_{\Lambda}\text{H}$ (left panel), ${}^4_{\Lambda}\text{H}$ (middle panel), and ${}^4_{\Lambda}\text{He}$ (right panel). The dotted lines represent exponential fits to the data.

26 In 2018, data from Au+Au collisions at $\sqrt{s_{NN}} = 3.0$ GeV and 7.2 GeV have been collected,
 27 with 258 and 155 million recorded events respectively. The lifetime analyses were
 28 carried out for ${}^3_{\Lambda}\text{H}$ and ${}^4_{\Lambda}\text{H}$ using both data sets, while the ${}^4_{\Lambda}\text{He}$ analysis utilized the $\sqrt{s_{NN}} =$
 29 3.0 GeV dataset only. In order to extract the lifetime, the hypernuclei yields are measured
 30 as a function of proper decay length. As shown in Fig. 1, the resultant distributions are well
 31 described by exponential functions.

32 The lifetimes are extracted via χ^2 fits with exponential functions. As a cross-check,
 33 the lifetime of the Λ is extracted using the same method and the measured lifetime,
 34 $267 \pm 1(\text{stat}) \pm 4(\text{syst})$ ps, is consistent with the PDG value [1]. Four major sources of
 35 systematic uncertainties are considered. They include imperfect description of topological
 36 variables in the GEANT simulations for efficiency estimation, imperfect knowledge of the
 37 true kinematic distribution of the hypernuclei, the simulated TPC tracking efficiency, and the
 38 signal extraction technique. Their contributions are estimated by varying topological cuts
 39 for hypernuclei candidate selection, the hypernuclei transverse momentum p_T and rapidity
 40 y distributions in the GEANT simulations, the TPC track quality selection criteria, and the
 41 background subtraction method. Other effects, such as particle misidentification, contami-
 42 nation from three-body decays, and coulomb dissociation through target material, have been
 43 quantified via Monte-Carlo simulations and are negligible compared to other sources of un-
 44 certainty. Different sources of systematic uncertainties are assumed to be uncorrelated and

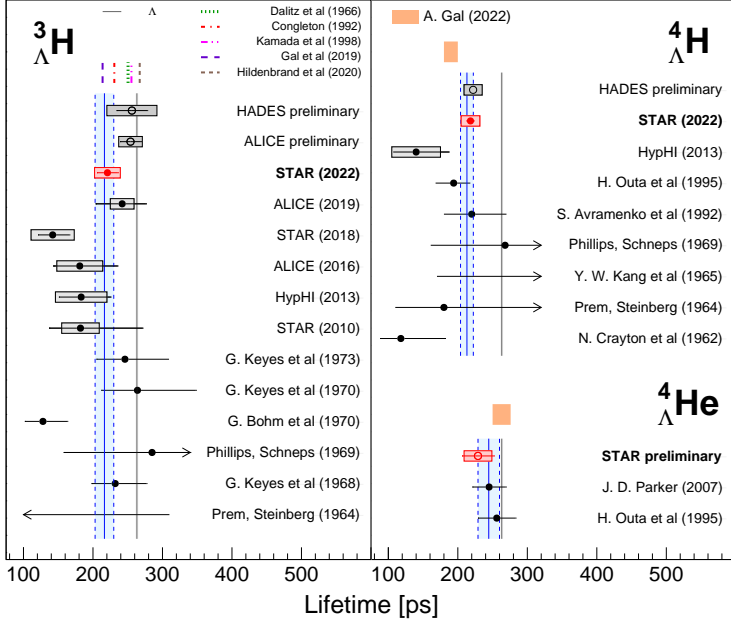


Figure 2. Compilation of ${}^3_{\Lambda}\text{H}$, ${}^4_{\Lambda}\text{H}$ and ${}^4_{\Lambda}\text{He}$ lifetimes. The experimental average lifetimes are indicated by blue shaded bands. The short dashed lines and solid bands represent theoretical calculations while the solid grey line indicates the free Λ lifetime.

45 added in quadrature. The total systematic uncertainty amounts to 8.2%, 6.0%, and 8.7% for
 46 ${}^3_{\Lambda}\text{H}$, ${}^4_{\Lambda}\text{H}$, and ${}^4_{\Lambda}\text{He}$ respectively.

47 The ${}^3_{\Lambda}\text{H}$, ${}^4_{\Lambda}\text{H}$, and ${}^4_{\Lambda}\text{He}$ lifetimes are measured to be $221 \pm 15(\text{stat}) \pm 19(\text{syst})$ ps,
 48 $218 \pm 6(\text{stat}) \pm 13(\text{syst})$ ps [5], and $229 \pm 23(\text{stat}) \pm 20(\text{syst})$ ps respectively. In Fig. 2,
 49 the results are compared to published measurements, preliminary results from ALICE [6]
 50 and HADES [7], and theoretical calculations. The experimentally averaged ${}^3_{\Lambda}\text{H}$ lifetime is
 51 $(82 \pm 5)\%$ of the Λ lifetime, consistent with theoretical calculations incorporating pion final-
 52 state interactions [8]. Similar to the ${}^3_{\Lambda}\text{H}$, the experimental averages of ${}^4_{\Lambda}\text{H}$ and ${}^4_{\Lambda}\text{He}$ lie below
 53 the Λ lifetime. Their ratio $\tau_{\text{avg}}({}^4_{\Lambda}\text{H})/\tau_{\text{avg}}({}^4_{\Lambda}\text{He})$ is equal to 0.85 ± 0.07 , compatible with theo-
 54 retical estimates invoking the isospin rule [9], which is based on the experimentally measured
 55 ratio, $\Gamma(\Lambda \rightarrow n + \pi^0)/\Gamma(\Lambda \rightarrow p + \pi^-) \approx 0.5$. The new ${}^3_{\Lambda}\text{H}$ and ${}^4_{\Lambda}\text{H}$ results from STAR have
 56 an improved precision compared to previous measurements, providing stronger constraints to
 57 hyperon-nucleon interaction models.

58 4 Relative Branching Ratio of the Hypertriton

The ${}^3_{\Lambda}\text{H}$ relative branching ratio R_3 , defined as:

$$R_3 = \frac{BR({}^3_{\Lambda}\text{H} \rightarrow {}^3\text{He} + \pi^-)}{BR({}^3_{\Lambda}\text{H} \rightarrow {}^3\text{He} + \pi^-) + BR({}^3_{\Lambda}\text{H} \rightarrow \text{d} + \text{p} + \pi^-)}, \quad (1)$$

59 where BR stands for branching ratio, is an important input to theoretical computations of
 60 the ${}^3_{\Lambda}\text{H}$ lifetime. Calculations has shown that the two-body and three-body mesonic decay
 61 channels of the ${}^3_{\Lambda}\text{H}$ contribute $\sim 97\%$ of the total decay rate [10], while the remaining $\sim 3\%$

62 stems from four-body mesonic decays and non-mesonic decays. Since the π^- decay rate and
 63 the π^0 decay rate are related to each other via the isospin rule, the lifetime of the ${}^3_{\Lambda}\text{H}$ can
 64 be estimated via a hybrid method: theoretically computing the ${}^3_{\Lambda}\text{H} \rightarrow {}^3\text{He} + \pi^-$ decay rate
 65 and combining with the experimentally determined R_3 [11]. Thus, the ${}^3_{\Lambda}\text{H}$ R_3 provides an
 66 additional handle to access its lifetime.

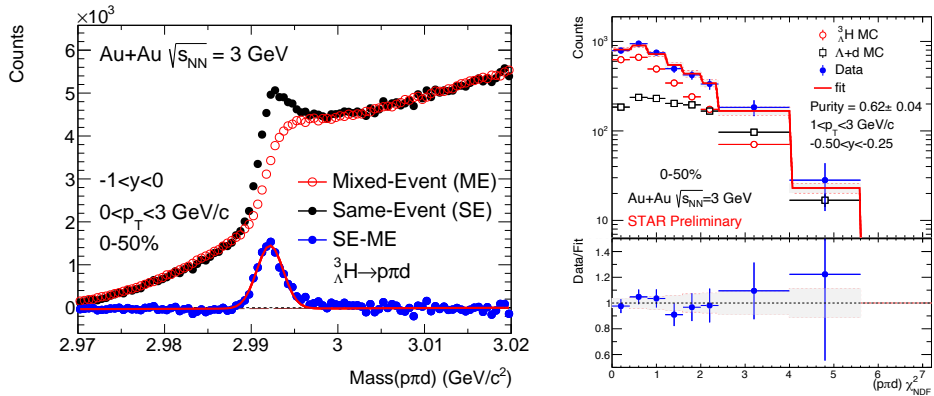


Figure 3. (left) Invariant mass of $d-p-\pi^-$ triplets from Au+Au collisions at $\sqrt{s_{NN}}=3.0$ GeV. Data are shown as solid black markers, the combinatorial background estimated via event mixing is shown as the open red markers, and the background subtracted distribution is shown as the solid blue markers. (right, upper panel) Template fit to χ^2 of the secondary vertex fit. The solid blue markers represent the data after combinatorial background subtraction, red and black open markers represent contributions from signal and correlated background respectively. The solid red line indicates the sum of the components. (right, bottom panel) Ratio of the data after combinatorial background subtraction to the sum of the components.

67 The ${}^3_{\Lambda}\text{H}$ yields are measured in $\sqrt{s_{NN}} = 3.0$ GeV Au+Au collisions via both two-body
 68 and three-body decay channels. The extraction of ${}^3_{\Lambda}\text{H}$ signal via its three-body decay is more
 69 complicated compared to the two-body decay due to significant contributions of correlated
 70 background in its invariant mass spectrum. As demonstrated in Fig. 3, after subtracting the
 71 combinatorial background which is estimated via event-mixing, a template fit is applied to
 72 the data to statistically separate contributions from correlated background and signal. The fit
 73 exploits the fact that, for true ${}^3_{\Lambda}\text{H}$ signal, all three daughter tracks point to the same secondary
 74 vertex, which gives rise to smaller χ^2 values in the secondary vertex fit, while correlated
 75 background does not, and lead to larger χ^2 values.

76 By comparing the corrected yields from the two decay channels, R_3 can be determined.
 77 The preliminary result $R_3 = 0.27 \pm 0.03(\text{stat}) \pm 0.04(\text{syst})$, as shown in Fig. 4, is consistent
 78 with previous measurements. Our new measurements provide improved precision to the ${}^3_{\Lambda}\text{H}$
 79 R_3 , which, aside from its connection to the lifetime, may also provide constraints on its
 80 binding energy [11].

81 5 Summary and Outlook

82 In summary, recent studies on hypernuclei lifetimes and branching ratios from STAR have
 83 been discussed. New lifetime measurements of ${}^3_{\Lambda}\text{H}$, ${}^4_{\Lambda}\text{H}$, and ${}^4_{\Lambda}\text{He}$ from the Beam Energy Scan
 84 II program have been presented. In particular, the new ${}^3_{\Lambda}\text{H}$ and ${}^4_{\Lambda}\text{H}$ lifetime measurements are
 85 the most precise published results to date, providing strong constraints to hyperon-nucleon

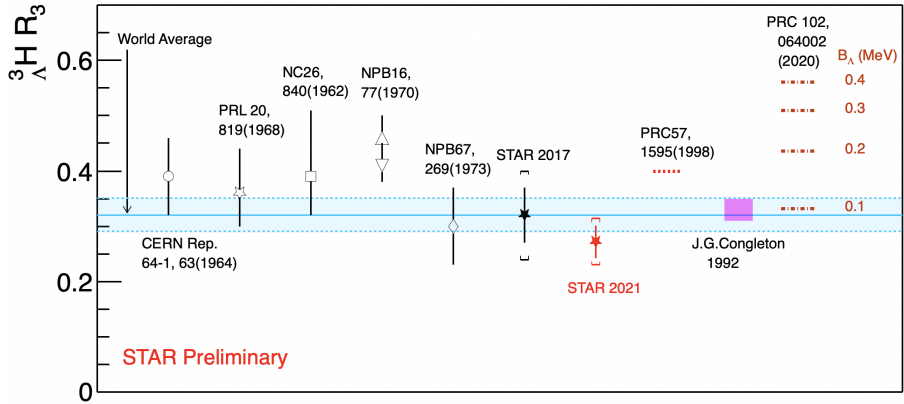


Figure 4. Compilation of ${}^3_{\Lambda}\text{H}$ relative branching ratio R_3 . The experimental average R_3 is indicated by the blue shaded band. The magenta box and dashed red and orange lines represent theoretical calculations.

86 interaction models. In addition, the ${}^3_{\Lambda}\text{H}$ relative branching ratio R_3 has been extracted in $\sqrt{s_{NN}}$
 87 $= 3.0$ GeV Au+Au collisions. The improved precision on R_3 provides the necessary input for
 88 connecting theoretically computed two-body mesonic decay rates and the ${}^3_{\Lambda}\text{H}$ lifetime.

89 References

- 90 [1] P. Zyla et al. (Particle Data Group), Prog. Theor. Exp. Phys. 2020, 083C01 (2020)
 91 [2] A. Andronic et al., Phys. Lett. B **697**, 203 (2011), (update, preliminary)
 92 [3] I. Kisel (CBM, STAR collaborations), J. Phys. Conf. Ser. **1602**, 012006 (2020).
 93 [4] J. Adam et al. (STAR collaboration), Phys. Rev. C **102**, 034909 (2020)
 94 [5] M. S. Abdallah et al. (STAR collaboration), Phys. Rev. Lett. **128**, 202301 (2022)
 95 [6] E. Bartsch (ALICE collaboration), Nucl. Phys. A **1005**, 121791 (2021)
 96 [7] S. Spies (HADES collaboration), these proceedings
 97 [8] A. Gal and H. Garcilazo, Phys. Lett. B **791**, 48 (2019)
 98 [9] A. Gal, EPJ Web Conf. **259**, 08002 (2022)
 99 [10] H. Kamada et al., Phys. Rev. C **57**, 1595 (1998)
 100 [11] F. Hildenbrand and H.-W. Hammer, Phys. Rev. C **102**, 064002 (2020)